Transactions, **SMiRT-26**
Berlin/Potsdam, Germany, July 10-15, 2022
Division V

IMPACT TESTING IN VTT

Alexis Fedoroff[1], Kim Calonius[1], Ari Vepsä[1], Arja Saarenheimo[1]

[1] VTT Technical Research Centre of Finland Ltd, Espoo, Finland (firstname.lastname@vtt.fi)

ABSTRACT

Structural integrity of nuclear power plant components and structures is of paramount importance in external hazard events for safe process shutdown. The purpose of the impact testing facility is to investigate experimentally the possible outcomes of airplane crash scenarios. For almost two decades, VTT has conducted impact tests with various projectiles and targets with the aim of perfectioning the testing equipment and measurement methods. The next phase in this upgrade process consists in a larger scale test facility, which will enable the study of geometric scale effects on impact tests. The fundamental research question that motivates this scale effect study is whether the research results obtained during decades of testing are still valid in a full scale airplane crash scenario. As a bonus, the new test facility can also be fitted to carry out inclined impacts and shock wave tests on concrete structures.

INTRODUCTION

In the direct aftermath of 9/11 it was recognized by the Finnish nuclear safety authority that there is a need for thorough understanding of the behaviour of NPP concrete structures under airplane crash scenario. The Technical Research Centre of Finland (VTT) was given the task to develop an experimental test setup for impact testing. Now, two decades later, hundreds of impact tests have been carried out with the original VTT impact test apparatus in multiple international projects and a vast amount of knowledge is accumulated. It is, however, recognized that there are new research topics in structural integrity that must be addressed, which is the reason why VTT decided to upgrade the impact test facility. The upgraded facility, ready for use in 2023, enables the experimental study of impact tests at various geometric scales, various inclination angles and enables the use of the impact facility also as a shock wave tube. In conjunction with the second generation impact tests, VTT also proposes an upgraded selection of measurement methods, both to quantify the impact test response and in order to characterize material behaviour.

TEST METHODS

In an airplane crash scenario, various buildings in a NPP respond differently to each part of the airplane. Turbine shafts and landing gears create local punching damage, whereas the folding fuselage induces detrimental vibrations in the entire building. Fuel tanks also induce both mechanical and deflagration damage. The objective of experimental impact studies is to isolate separate damage modes to investigate the structural response to a given type of impactor on a scaled model. Various type of projectiles may be used as impactors: non-deformable hard projectiles that create local punching damage (Figure 1) and deformable soft projectiles that create global bending damage induced by the folding mechanism (Figure 2). In addition, one has semi-hard projectiles that create both local shear and global bending damage (Figure 3). In vibration propagation studies (Figure 4), a soft projectile induces global vibrations in the structure, and in liquid filled projectile tests (Figure 5) one can study the effect of fuel splash. In a crash scenario on the rooftop, the impact angle plays an important role, which can be studied in inclined tests (Figure 6).

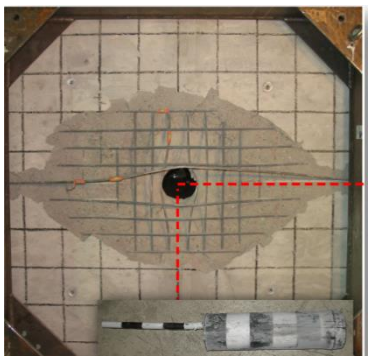

Figure 1.

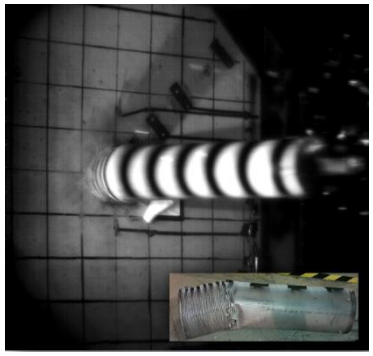

Figure 2.

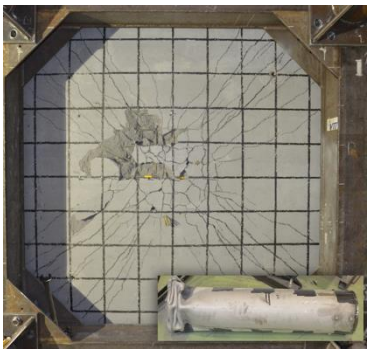

Figure 3.

Figure 4.

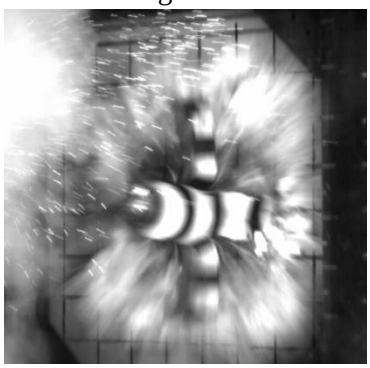

Figure 5.

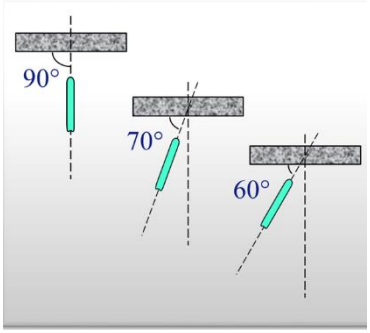

Figure 6.

MEASUREMENT METHODS

An important number of various measurement types is available for impact testing, both real-time and post-impact ones. Since the duration of an impact is typically 10-20ms, all real-time data acquisition is implemented with high frequency A/D sampling cards that are connected to a National Instruments PXI-type computer with a capacity for up to 48 channels with extra room for additional data acquisition cards. In impact tests, real-time data consists in strain measurements on reinforcement and concrete surface, displacement and acceleration measurements of selected points on the structure, force measurements at target structure supports and laser measurements to determine projectile impact velocity. In addition, there are multiple high-speed cameras are placed at different angles to capture a video footage of the impact at rates of 1500 to 7500 frames per second (Figure 7). The video footage can be later analysed frame by frame in a CAD software (Figure 8) to produce a reliable measurement of the projectile translational and angular position during impact. Such a kinematic analysis enables the determination of the velocity profile, including residual velocity, in a hard projectile test and the determination of crushing and sliding velocities in a soft projectile test.

Besides the real-time measurements, impact tests also involve tests to determine material parameters, and post-impact measurements to quantify the extent of damage in the concrete structure and the failure mode. The standard material test matrix used in impact test, which consists in uniaxial monotonic and cyclic compression tests on concrete specimens, both force driven and displacement driven, triaxial compression tests at different confinement ratio, three point bending tests on notched concrete beam as well as split tensile tests. For reinforcement steel material and projectile steel material tensile tests are performed at multiple strain rates. As a result, main concrete parameters (concrete tensile and compressive strength, fracture energy, secant stiffness modulus, stiffness degradation, triaxial strength properties) as well as main steel parameters (yield/proof stress, maximum stress, ultimate elongation, strain rate sensitivity) are determined.

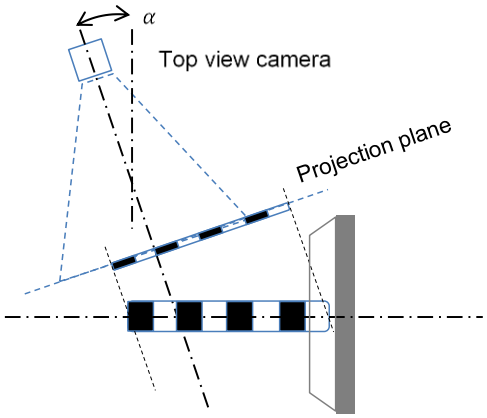

Figure 7. Schematic view of high-speed camera placement

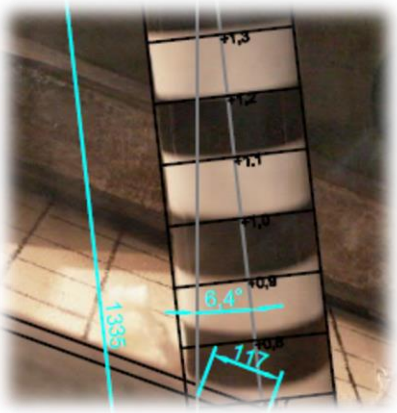

Figure 8. Translational and angular position determination in CAD software

Post-impact measurements typically include photographs of the slab cracking pattern, determination of the area of scabbed and spalled concrete as well as the mass of loose concrete after impact. Deformation measurements of the projectile as well as permanent deformations of the target structure belong to the standard set of measurements. Section views of the damaged structure are produced using a diamond cutting disc. Novel post-impact measurement methods, including target structure vibration mode measurement as well as target structure 3D scan of surface and ultrasonic scan for internal defect recognition are currently under investigation.

RESEARCH FACILITY

The VTT old (1st generation) impact test apparatus is shown in Figure 9 and views of the upgraded new (2nd generation) test facility are shown in Figure 10. The apparatus uses pressurized air to accelerate the projectile to its target velocity. Contrary to the old test facility, the upgraded test facility is designed to fit different geometric scales and due to a modular approach in the design, it can be adapted in the future to a large number of testing scenarios. Table 1 shows the capacity of the test facility.

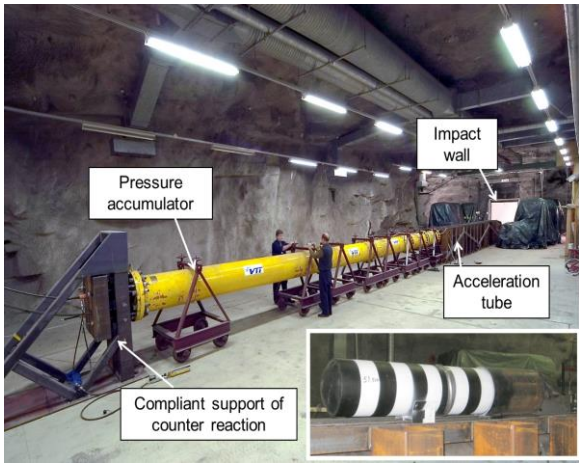

Figure 9. Old test facility

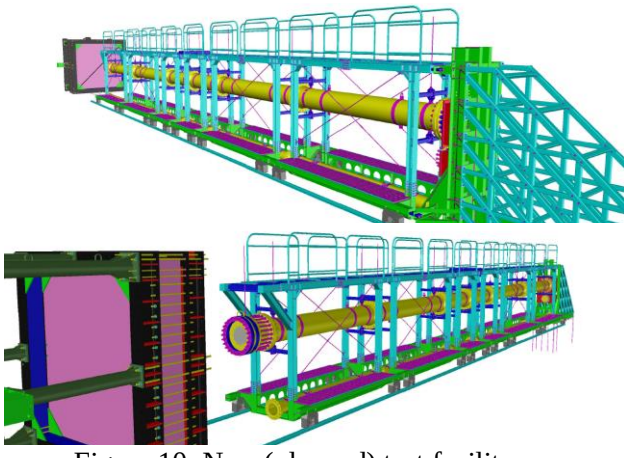

Figure 10. New (planned) test facility

Table 1: Comparison of 1st and 2nd generation impact test facility capabilities

	1st generation test facility (old)	2nd generation test facility (planned)	
		reference scale	larger scale
geometric scale factor	1.0	1.0	1.75
projectile mass	50 kg	50 kg	270 kg
max. impact speed	170 m/s	200 m/s	165 m/s
target slab size	2.0 m by 2.0 m	2.0 m by 2.0 m	3.5 m by 3.5 m
max. target slab thickness	350 mm	350 mm	440 mm
max. shooting pressure	20 bar	25 bar	25 bar
limit pressure	50 bar	50 bar	50 bar
pressurized air volume	0.84 m3	2.1 m3	2.1 m3
max. side-on overpressure	N/A	N/A	8.5 bar

EVALUATION OF SHOOTING PRESSURE VS. SHOOTING VELOCITY RELATION

One of the issues of paramount importance in impact testing is correct prediction of impact velocity as a function of shooting pressure P_0. At time $t = 0$ pressurized air of a total volume V_0 is accumulated behind a membrane. After the burst of the membrane, pressurized air is released, and the projectile is pushed forward with a pressure $P(t)$. The pressure is rapidly decreasing due to an increase in air volume, $V(t) = V_0 + V_1\, x(t)/L$, and the lost air flow $m_{\text{out}}(t)$ through openings in the acceleration tube. In the old test facility, the projectile is placed above the acceleration tube and is pushed by a piston placed inside the acceleration tube (Figure 11). In the new test facility, the projectile is placed inside the acceleration tube, which considerably reduces the amount of lost air flow (Figure 12).

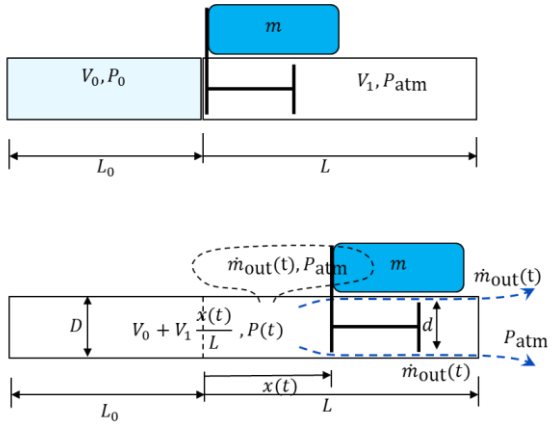

Figure 11. Old test facility at initial and current time frame

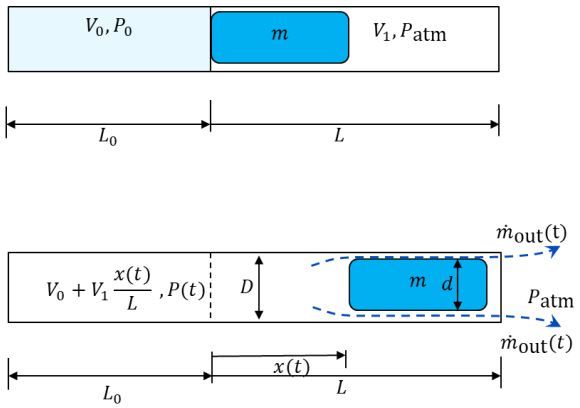

Figure 12. New test facility at initial and current time frame

At time $t = 0$, for an isentropic compression, the ideal gas law $P_0V_0 = n_0RT_0$ and the relation $T_0/T_{\text{atm}} = (P_0/P_{\text{atm}})^{(\gamma-1)/\gamma}$ gives the total number of moles in the system: $n_0 = V_0(P_0/P_{\text{atm}})^{1/\gamma}\, P_{\text{atm}}/(RT_{\text{atm}})$. Recall that for air $\gamma = c_{\text{p}}/c_{\text{v}} = 1.4$. Considering the ideal gas equation $P_{\text{atm}} = \rho_{\text{atm}}R_{\text{s}}T_{\text{atm}}$, one can write the total number moles in the system as follows: $n_0 = V_0(P_0/P_{\text{atm}})^{1/\gamma}\, \rho_{\text{atm}}/M$, where $M = 28.97$ g/mol

denotes the molar mass for air. If $n_{\text{out}}(t) = m_{\text{out}}(t)/M$ denotes the number of moles of air lost, then then number of moles of air available is $n(t) = n_0 - n_{\text{out}}(t)$. At time $t > 0$, the ideal gas law for the lost air is $P_{\text{atm}}V_{\text{out}}(t) = n_{\text{out}}(t)RT_{\text{atm}}$, and the ideal gas law for the available air is $P(t)V(t) = n(t)RT(t)$. Using the relation between pressure and temperature, $T(t)/T_0 = (P(t)/P_0)^{(\gamma-1)/\gamma}$, one gets $P(t)(V_0 + V_1\, x(t)/L)^{\gamma} = (1 - n_{\text{out}}(t)/n_0)^{\gamma} P_0 {V_0}^{\gamma}$, whence Equation (1).

$$\frac{P(t)}{P_0} = \left(\frac{1 - n_{\text{out}}(t)/n_0}{1 + (V_1/V_0)(x(t)/L)}\right)^{\gamma} \tag{1}$$

The equation of motion of the missile is $m\ddot{x}(t) = P(t)A_{\text{p}} - F_{\text{d}}(t)$, where $m = m_{\text{m}} + m_{\text{p}}$ denotes the total accelerated mass, $A_{\text{p}} = \pi {d_{\text{p}}}^2/4$ the cross-sectional area of the piston, $x(t)$ the position of the piston and $F_{\text{d}} = F_{\text{f}} + F_{\text{v}} + F_{\text{a}}$ the sum of all dissipative forces. The missile cross-sectional area is denoted $A_{\text{m}} = \pi {d_{\text{m}}}^2/4$, m_{m} and m_{p} are the masses of the missile and the piston, respectively. The frictional forces are $F_{\text{f}} = \mu g m$, where $\mu = 0.5$ denotes the coefficient of dry friction. The viscous forces are $F_{\text{v}} = \chi\, A_{\text{c}}/e_1\ \dot{x}(t)$, where A_{c} denotes the frictional contact area, e_1 the gap width and for air the coefficient of dynamic viscosity is $\chi = 18.4$ µPa·s. The air drag forces expression is $F_{\text{a}} = C_{\text{a}}A_{\text{a}}\rho_{\text{atm}}\,\dot{x}^2(t)/2$, where $C_{\text{a}} = 1.3$ denotes the air drag coefficient and A_{a} denotes the air drag area. The equation of motion is then given by Equation (2).

$$m\ddot{x}(t) = P(t)A_{\text{p}} - \mu g m - \chi\, A_{\text{c}}/e_1\ \dot{x}(t) - \tfrac{1}{2}C_{\text{a}}A_{\text{a}}\rho_{\text{atm}}\dot{x}^2(t) \tag{2}$$

The lost air mass is given by the choked mass flow rate equation, $\dot{m}_{\text{out}}(t) = \Gamma C_{\text{d}}A_{\text{d}}(t)\sqrt{P(t)\rho(t)}$, where C_{d} is the coefficient of discharge, $A_{\text{d}}(t)$ is the area of discharge, and $\Gamma = \sqrt{\gamma(2/(\gamma+1))^{(\gamma+1)/(\gamma-1)}}$. For isentropic conditions consider the relation $\rho(t) = (P(t)/P_{\text{atm}})^{1/\gamma}\rho_{\text{atm}}$, which can be substituted back into the choked mass flow rate equation. One gets Equation (3).

$$\dot{m}_{\text{out}}(t) = \Gamma C_{\text{d}}A_{\text{d}}(t)\sqrt{P_{\text{atm}}\rho_{\text{atm}}}\,(P(t)/P_{\text{atm}})^{(\gamma+1)/(2\gamma)} \tag{3}$$

Considering the shorthand notations $\xi(t) = x(t)/L$ and $\eta(t) = n_{\text{out}}(t)/n_0$ as well as $\alpha = V_1/V_0$, one gets $P(t) = P_0\big((1-\eta(t))/(1+\alpha\xi(t))\big)^{\gamma}$. Substitution into Equations (2) and (3) yields a pair of differential equations:

$$\begin{cases} \ddot{\xi}(t) &= \dfrac{P_0A_{\text{p}}}{mL}\left(\dfrac{1-\eta(t)}{1+\alpha\xi(t)}\right)^{\gamma} - \dfrac{\mu g}{L} - \chi\,\dfrac{A_{\text{c}}}{e_1 m}\,\dot{\xi}(t) - \dfrac{C_{\text{a}}A_{\text{a}}L\rho_{\text{atm}}}{2m}\dot{\xi}^2(t) \\ \dot{\eta}(t) &= \dfrac{\Gamma C_{\text{d}}A_{\text{d}}(t)\sqrt{P_{\text{atm}}/\rho_{\text{atm}}}}{V_0}\left(\dfrac{P_0}{P_{\text{atm}}}\right)^{(\gamma-1)/(2\gamma)}\left(\dfrac{1-\eta(t)}{1+\alpha\xi(t)}\right)^{(\gamma+1)/2} \end{cases} \tag{4}$$

If one defines the coefficients $K_1 = P_0A_{\text{p}}/(mL)$, $K_2 = \mu g/L$, $K_3 = \chi\, A_{\text{c}}/(e_1 m)$, $K_4 = C_{\text{a}}A_{\text{a}}L\rho_{\text{atm}}/(2m)$ as well as $K_5 = C_{\text{d}_1}A_{\text{d}_1}k_{\text{d}}$ and $K_6 = C_{\text{d}_2}A_{\text{d}_2}k_{\text{d}}$, with $k_{\text{d}} = \Gamma/V_0\,\sqrt{R_{\text{s}}T_{\text{atm}}}\,(P_0/P_{\text{atm}})^{(\gamma-1)/(2\gamma)}$, then one can write the differential Equation (4) in a canonical form:

$$\begin{cases} \dot{y}_1(t) &= y_2(t) \\ \dot{y}_2(t) &= K_1\big((1-y_3(t))/(1+\alpha y_1(t))\big)^{\gamma} - K_2 - K_3\, y_2(t) - K_4 {y_2}^2(t) \\ \dot{y}_3(t) &= \big(K_5 + K_6 y_1(t)\big)\big((1-y_3(t))/(1+\alpha y_1(t))\big)^{(\gamma+1)/2} \end{cases} \tag{5}$$

Table 2 shows the input data and specific expressions used to calculate the different acceleration tube cases.

Table 2: Expressions and input data for old and new acceleration tube

Expression	Old acceleration tube	New acceleration tube	
		Scale 1.00	Scale 1.75
missile mass m_{m}	50kg	50kg	268kg
piston mass m_{p}	50kg	8kg	43kg
missile diameter d_{m}	220mm	220mm	385mm
piston diameter d_{p}	490mm	288mm	565mm
piston length l_{p}	N/A	1000..2000mm	1750..3500mm
frictional contact area A_{c}	0	$\pi d_{\mathrm{p}} l_{\mathrm{p}}$	$\pi d_{\mathrm{p}} l_{\mathrm{p}}$
air drag cross-sectional area A_{a}	$A_{\mathrm{p}} + A_{\mathrm{m}}$	A_{p}	A_{p}
air drag coefficient C_{a}	1.30	0.50	0.50
piston to tube gap e_1	5mm	5mm	5mm
gap in tube e_2	10mm	0mm	0mm
Discharge area A_{d_1}	$\pi(d_{\mathrm{p}} + e_1)e_1$	$\pi(d_{\mathrm{p}} + e_1)e_1$	$\pi(d_{\mathrm{p}} + e_1)e_1$
Discharge area A_{d_2}	Le_2	0	0
Coefficient of discharge C_{d_1}	0.85	0.85	0.85
Coefficient of discharge C_{d_2}	5.00	N/A	N/A

Figure 13 shows the pressure-velocity curve for the old and new acceleration tube with data points from actual impact tests. For accelerated mass ($m_{\mathrm{m}}, m_{\mathrm{p}}$), a variation range of ±2% is imposed. For unknown parameters ($\mu, C_{\mathrm{a}}, C_{\mathrm{d}_1}, C_{\mathrm{d}_2}$), a variation range of ±20% is imposed.

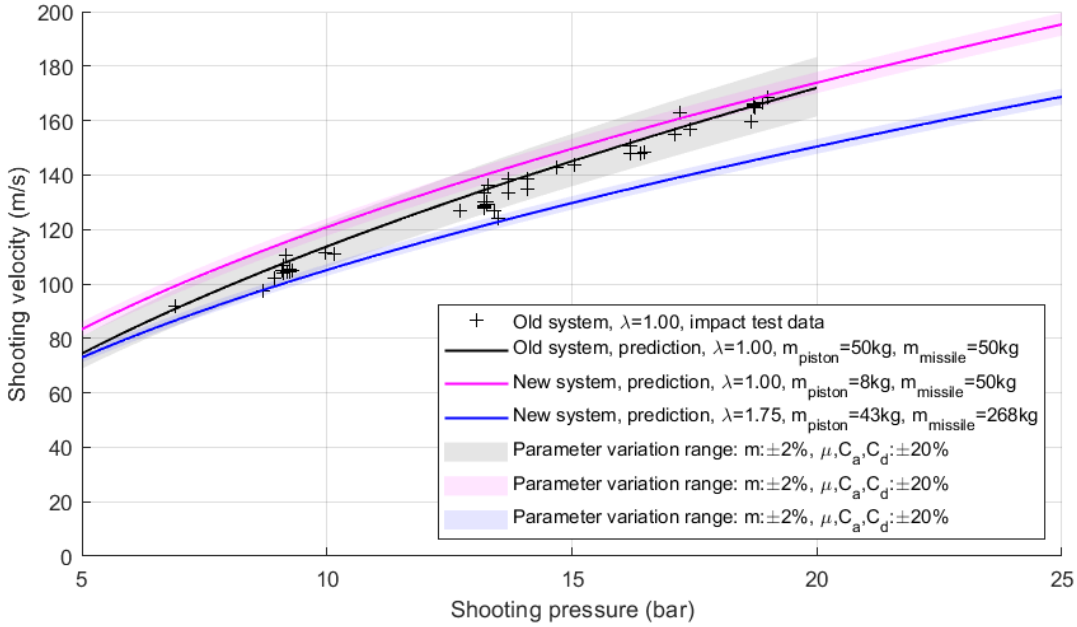

Figure 13. Pressure-velocity curve for old and new acceleration tubes

EVALUATION OF SHOCK WAVE OF PRESSURIZED AIR BURST

The new pressure tube and acceleration tube is designed to be used as a shock wave testing system as well. Figure 14 shows the layout principle. The tested component is connected to the shock wave tube by a conical adapter.

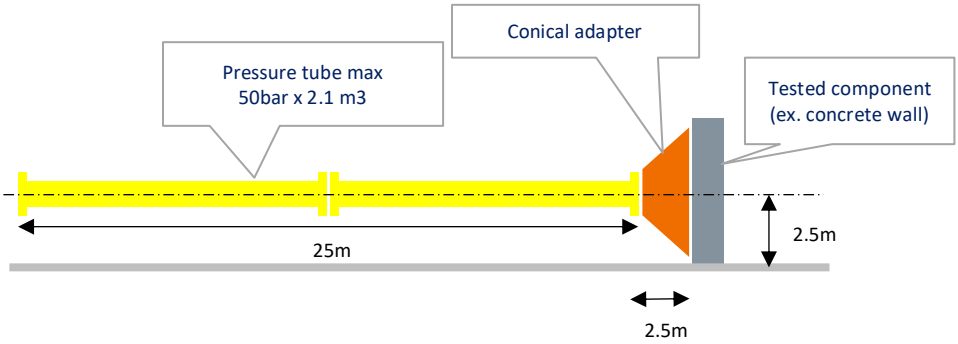

Figure 14. Impact tube used as shock wave testing system

To evaluate the capacity of such a system, one-dimensional shock wave theory is used to obtain the shock wave properties. It is considered that the compression is isentropic compression (no exchange of matter or energy). Hence, $T_1/T_{\text{atm}} = (P_1/P_{\text{atm}})^{(\gamma-1)/\gamma}$ gives $T_1/T_{\text{atm}} = 3.057877$, for $P_1 = 50$ bar. The sound wave velocity in air relates by the equation $a_1/a_{\text{atm}} = \sqrt{T_1/T_{\text{atm}}}$, which gives $a_{\text{atm}} = 343\ \text{m/s}$ and $a_1 = 600\ \text{m/s}$. First, one has to compute the peak shock overpressure directly in front of the explosion. Equation 6, as per 'Yellow Book' (2005), Eq. 7-12, gives the peak shock overpressure, P_{so}. Notice that since the shock wave tube uses compressed air, the ratio of specific heats, $\gamma = 1.4$, is the same for the compressed gas and the ambient gas, which is dry air.

$$\frac{P_1}{P_{\text{atm}}} = (1+\bar{p}_{\text{so}})\left(1 - \frac{(\gamma-1)(a_{\text{atm}}/a_1)\bar{p}_{\text{so}}}{\sqrt{2\gamma(2\gamma+(\gamma+1))\bar{p}_{\text{so}}}}\right)^{-2\gamma/(\gamma-1)} \quad , \quad \bar{p}_{\text{so}} = P_{\text{so}}/P_{\text{atm}} - 1 \tag{6}$$

In Equation 6, $P_1 = 50$ bar denotes the initial absolute pressure of the compressed gas, $P_{\text{atm}} = 1.01$ bar denotes the atmospheric pressure and $\bar{p}_{\text{so}}$ the non-dimensional peak shock pressure directly after burst. The result of Equation 6, after iteration, is $\bar{p}_{\text{so}} = 7.42$, whence the peak shock overpressure directly after burst is P_{so} =8.53 bar.

Then, to compute the side-on pressure (i.e. the pressure experienced by an object as a blast wave passes by), one can use the nomogram in Figure 15, taken from 'Yellow Book' (2005), Fig. 7.5. One needs, however, to determine first the peak target distance from explosion, r_{o} that corresponds to the peak shock overpressure directly after burst, P_{so}. The peak target distance from explosion is given by $r_{\text{o}} = (3V_{\text{g}}/(2\pi))^{1/3} = 1.00$ m as per 'Yellow Book' (2005), Eq. 7-10. To compute non-dimensional target distances, one needs to compute the energy of a compressed gas as it expands to atmospheric pressure is $E_{\text{av}} = (P_1 - P_{\text{atm}})\,V_{\text{g}}/(\gamma-1)$. The volume of the pressurized air for the tube in Figure 14 is $V_{\text{g}} = 2.07\ \text{m}^2$, and hence the energy is $E_{\text{av}} = 25.31$ MJ. The effective blast wave energy is $E_{\text{ex}} \approx 1.0E_{\text{av}}$ when there is no ground reflection present. The non-dimensional peak target distance is $\bar{R}_{\text{o}} = r_{\text{o}}(P_{\text{atm}}/E_{\text{ex}})^{1/3} = 0.16$ as per 'Yellow Book' (2005), Eq. 7-11. From Figure 15, one can identify the point $(\bar{R}_{\text{o}}, \bar{p}_{\text{so}}) = (0.16\ ,7.42)$, which intersects the dashed blue curve.

To read the side-on pressure values, $\bar{p}_s$, from Figure 15, one has to evaluate first the non-dimensional target distances $\bar{R}_t$ from the distances $r_t = 1.50, 2.00, 2.50, \ldots$ m. Hence, one has $\bar{R}_t = r_t(P_{atm}/E_{ex})^{1/3} = 0.24, 0.32, 0.40, \ldots$ as per 'Yellow Book' (2005), Eq. 7-8. From Figure 15 one can read the non-dimensional side-on pressures $\bar{p}_s = 4.5, 3.2, 2.3, \ldots$ which correspond to the actual side on pressures $P_s = 5.6, 4.3, 3.3, \ldots$ bar. Likewise, one can read from Figure 15, as per 'Yellow Book' (2005), Fig. 7.10, the non-dimensional impulses $\bar{\imath}_{so} = 0.41$ and $\bar{\imath}_s = 0.22, 0.15, 0.12 \ldots$, which corresponds to the impulses $i_{so} = \bar{\imath}_{so} {P_{atm}}^{2/3} {E_{ex}}^{1/3}/a_{atm} = 763$ Pa·s and $i_s = \bar{\imath}_s {P_{atm}}^{2/3} {E_{ex}}^{1/3}/a_{atm} = 409, 279, 223, \ldots$ Pa·s.

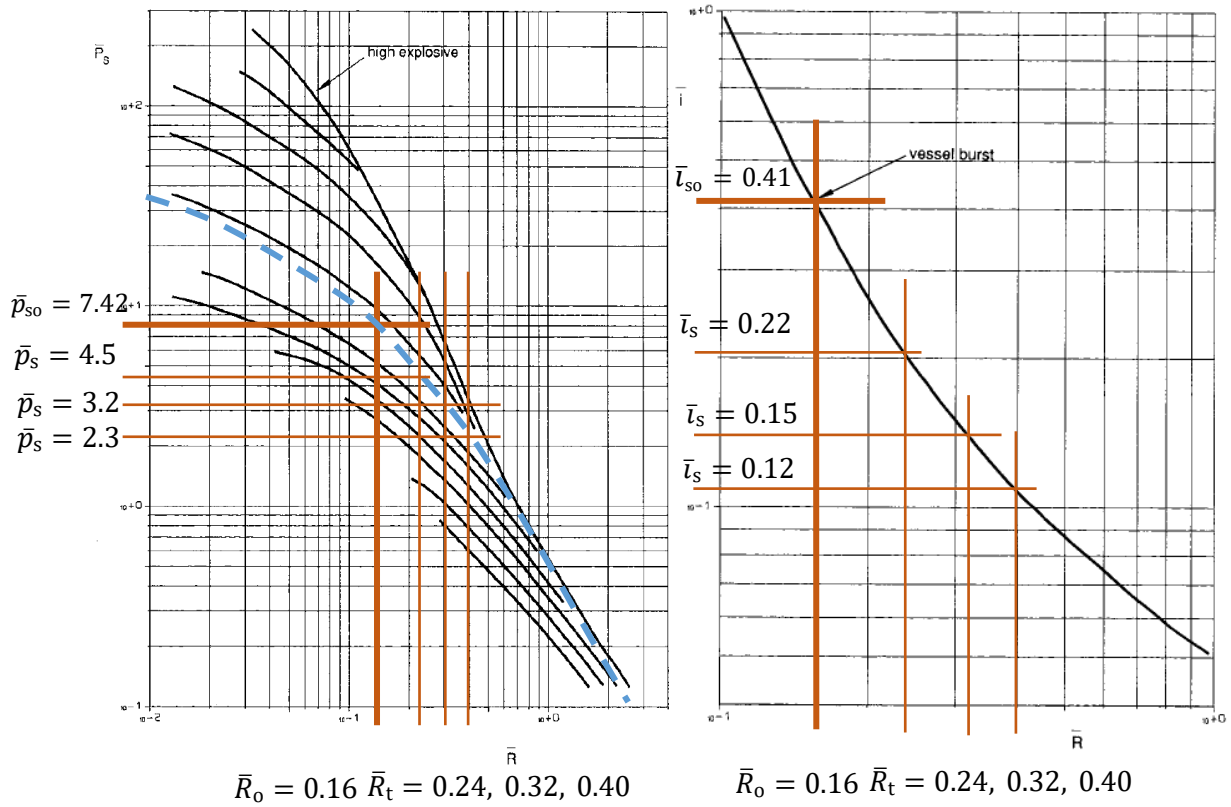

Figure 15. Impact tube used as shock wave testing system, Baker et al. (1978)

The target distances from explosion point versus side-on overpressures and impulses are plotted in Figure 16. Notice, however, that when the shock wave strikes a structure surface, it is reflected. The reflected pressure, P_r, and the reflected impulse, i_r, depends on the strength of the incident wave and reflection angle. If one considers a normal reflection in air, the reflected pressure may be maximally about 8 times the side-on pressure of the shock wave for ideal gases.

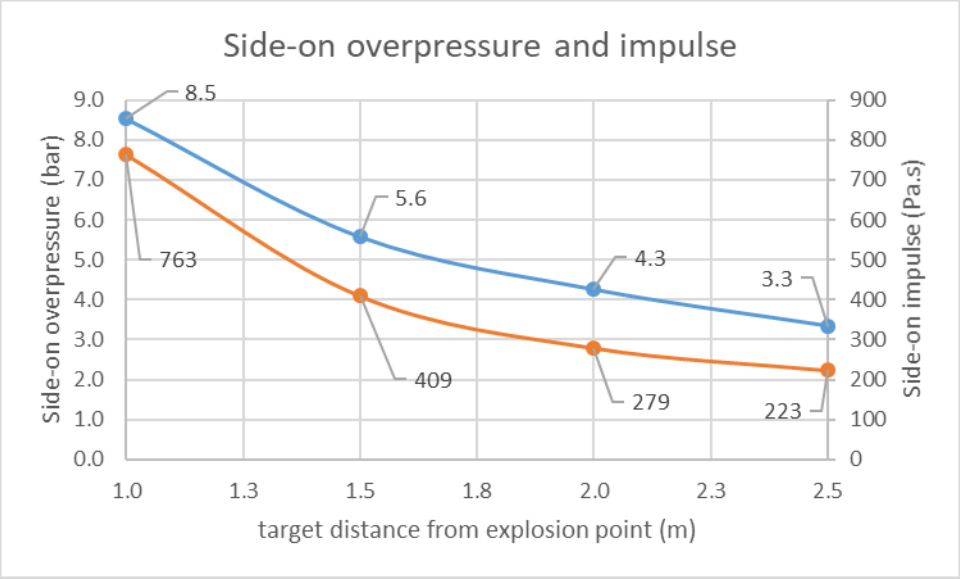

Figure 16. Side-on overpressure and impulse plot

SUMMARY AND REMARKS

The impact testing program in VTT is presented, and the impact testing apparatus is described. Currently, VTT is upgrading the impact test apparatus in order to get a platform for a larger variety of tests as compared to the past test facility. Among other, capability for larger scale tests, inclined tests as well as the double use of the test apparatus both for impact testing and shock wave testing is planned. Calculations to evaluate the shooting pressure vs. the shooting velocity are proposed as well as calculations to evaluate the side-on overpressure vs. target distance. Based on these calculations adequate design drawings of the upgraded impact test facility are implemented.

In order to participate to the impact related research, there is a wide range of possibilities. Currently, VTT is looking forward to find new participants for the three year jointly funded (shared benefit) project IMPACT phase V starting from year 2025. This future jointly funded project will be in the continuation line of the previous IMPACT phases I-IV. The content of IMPACT projects consists in fundamental and applied open research topics in the field of structural integrity. The tests are done in VTT and the results are shared between the participants. For applied research and development of impact and shock wave related topics VTT is proposing a wide range of services that can be purchased on a commercial basis. Finally, the VTT impact team is looking forward to participate in any future research consortium in the fields of structural integrity in the nuclear power plant or other critical infrastructure domain.

REFERENCES

Baker, W. E., Kulesz, J.J. et al. (1978). *Workbook for estimating the effects of accidental explosions in propellant handling systems*, NASA Contractor report no. 3023, NASA Scientific and Technical Information Office, Washington D.C.

'Yellow Book': Methods for the calculation of physical effects due to releases of hazardous materials (2005). Publicatiereeks gevaarlijke stoffen, The Hague. Editors: van den Bosch, C.J.H. and Weterings, R.A.P.M.